Journal of Applied Polymer Science

The electrostatic self-assembly of microgels on polymer brushes and its effects on interfacial friction

Ran Zhang,[1,2] Shuanhong Ma,[1,2] Guoqiang Liu,[1] Meirong Cai,[1] Qian Ye,[1] Bo Yu,[1] Feng Zhou[1]

[1]State Key Laboratory of Solid Lubrication, Lanzhou Institute of Chemical Physics, Chinese Academy of Sciences, Tianshui Middle Road, Lanzhou 730000, People's Republic of China

[2]University of Chinese Academy of Sciences, Beijing 100049, People's Republic of China

Correspondence to: Q. Ye (E-mail: yeqian213@licp.cas.cn) or B. Yu (E-mail: yubo@licp.cas.cn) or F. Zhou (E-mail: zhouf@licp.cas.cn)

ABSTRACT: In this article, a series of monodisperse poly(*N*-isopropylacrylamide-*co*-acrylic acid) [P(NIPAm-AA)] microgels were prepared with different content of acrylic acid (AA) by surfactant-free emulsion polymerization, and their electrostatic self-assemble and tribological behavior on polymer brushes were investigated. The ζ-potential of microgels became more negative with the increase content of AA, which means a stronger hydration capability. For cationic poly[2-(methacryloyloxy)ethyltrimethylammonium chloride] (PMETAC) brushes, negative P(NIPAm-AA) microgels adsorbed on the surfaces of brushes as a result of the electrostatic interaction, and more AA content means stronger absorption ability. However, compared to the polymer brushes, $P(NIPAm\text{-}AA)_{2:1}$ and $P(NIPAm\text{-}AA)_{5:1}$ microgels possessed the weaker hydration capability, which led to a concomitant increase in friction of interface. In terms of $P(NIPAm\text{-}AA)_{10:1}$ microgels, due to the weak adsorption, they could be sheared off easily, leading to the PMETAC brushes swell again, and thus, a lower friction of interface was obtained. Moreover, the tribological behavior of microgels was significantly affected by the pH, especially the $P(NIPAm\text{-}AA)_{2:1}$ microgels exhibited good lubrication property in high pH solution due to high hydration of deprotonated carboxylic acid groups. © 2016 Wiley Periodicals, Inc. J. Appl. Polym. Sci. **2016**, *133*, 44215.

KEYWORDS: friction; hydrophilic polymers; microgels; wear and lubrication

Received 7 April 2016; accepted 17 July 2016

DOI: 10.1002/app.44215

INTRODUCTION

Hydrogel particles (microgels) have been extensively studied in decades due to their intelligent response to external stimuli. It is well known that microgels are spherical, cross-linked polymeric networks that fully swollen in water.[1,2] One of the most important character for microgels is their thermosensitivity, while they are swollen at room temperature and shrunken above the volume phase transition temperature.[3] As a kind of typical soft matter, microgel particles have a range of potentially important applications.[4,5] Through rational design, their chemical and physical properties can be reversible regulated by changing the ambient conditions, for instance, pH,[6] temperature,[7] ionic strength,[8] quality of solvent[9] and the action of the external field.[10,11]

Microgels composed of poly(*N*-isopropylacrylamide) (PNIPAm) are perhaps the most investigated microgels and exhibit a lower critical solution temperature (LCST) around ~31 °C in aqueous media.[12,13] PNIPAm exhibits chains conformation transition above or below LCST, which is often used to change surface macroscopic properties,[5] such as frictional force and wettability.[14–16] Chang *et al.*[17] have prepared the stimulus-responsive PNIPAm hydrogels and found that the phase state of PNIPAm gels strongly influenced the friction coefficients under different shear rate. The PNIPAm hydrogel in a collapsed, hydrophobic state (above the LCST) exhibits obviously higher friction than swollen, hydrophilic gel (below the LCST) at low shear rates. Based on dissipative theory, the specific lubrication mechanisms responsible for PNIPAm hydrogels are discussed in detail. Jiang and coworkers have synthesized PNIPAm thin films through surface-initiated atom transfer radical polymerization (SI-ATRP), and the films exhibited different wettability under different temperature and surface roughness.[16] Reversible switch between superhydrophilicity and superhydrophobicity was realized in a narrow temperature range, and relative application of oil/water separation was presented in their research.

On the basis of microgel particles response performance, great attentions were paid to microgel modified surfaces during the past few years.[6,18–21] Klitzing and coworkers have prepared thermosensitive films by deposition of densely packed P(NIPAm-*co*-AA) microgels monolayer, and the impact of testing conditions on adsorption density of microgels was discussed in detail,

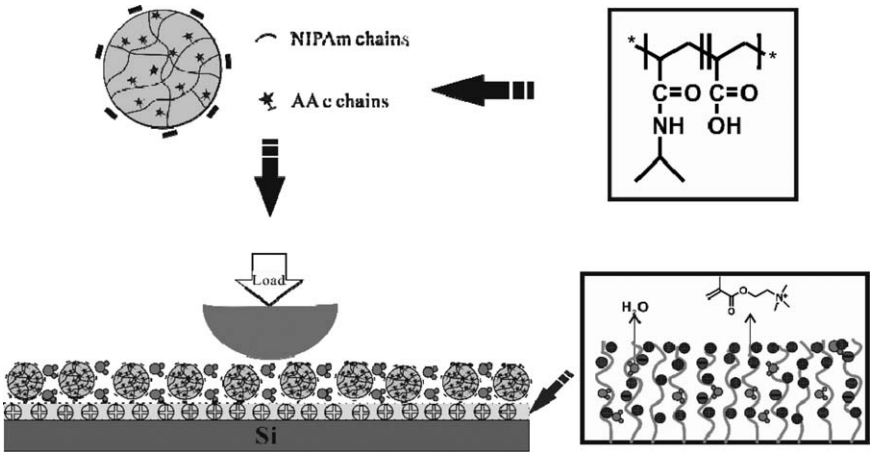

Figure 1. Schematic diagram of the electrostatic interaction between polymer brushes and oppositely charged microgels.

especially environmental pH.[6] It is well known that the acrylic acid (AA) units will become more charged with the increasing pH, which results in the microgel particles repell each other with a lower packing density. In addition, Serpe *et al.*[18] constructed P(NIPAm-*co*-AA) microgel thin films via layer-by-layer deposition and found that the microgel films exhibited enhanced thermoresponsivity blow p*K*a of the microgel AA groups. More importantly, microgels can be assembled into various 2D or 3D nanostructures, which also has great potential for sensing and biomedical applications.[20]

In this article, poly(*N*-isopropylacrylamide-*co*-acrylic acid) [P(NIPAm-AA)] microgels with different contents of AA were synthesized via surfactant-free emulsion polymerization. It is obvious that the ζ-potential of microgels became more negative with the increase content of AA, which means a better hydration capability. Furthermore, the electrostatic interaction between positive poly[2-(methacryloyloxy)ethyltrimethylammonium chloride] (PMETAC) brushes and negative P(NIPAm-AA) microgels was investigated, and this kind of electrostatic attraction made plenty of microgels adsorb on the surface of polymer brushes and therefore affected interfacial friction as shown in Figure 1. For $P(NIPAm\text{-}AA)_{2:1}$ and $P(NIPAm\text{-}AA)_{5:1}$ microgels, the weaker hydration capability compared to polymer brushes led to a concomitant increase in friction of interface, however, they could be sheared off by heavier load or higher frequency. In terms of $P(NIPAm\text{-}AA)_{10:1}$ microgels, due to the weak adsorption, they could be sheared off easily under the load of 0.5 *N*; thus, the PMETAC brushes swelled again and resulted in a lower friction of interface.

EXPERIMENTAL

Materials

2-(Methacryloyloxy)ethyltrimethylammonium chloride (METAC, 80% in water; TCI Shanghai, Shanghai, China), *N*-isopropylacrylamide (NIPAm, 99%; J&K, Beijing, China), and AA (Sigma-Aldrich China, Shanghai, China) were used as received. The cross-linker *N*,*N*′-methylenebisacrylamide (BIS) and the initiators potassium persulfate (KPS) and 2,2′-Bipyridyl (bipy; analytically pure) were commercially available and used without any purification. Copper (I) bromide was purified by heating reflux overnight in acetic acid. 3-(Trichlorosilyl)propyl-2-bromo-2-methylpropanoate (SI-ATRP initiator) was synthesized according to previous reports.[22,23]

Synthesis of P(NIPAm-AA) Microgels with Different Charge Density

A series of monodisperse P(NIPAm-AA) microgels with different contents of AA were synthesized by surfactant-free emulsion polymerization. The general procedures are described in the following: NIPAm (1.0 g, 1.0 wt %), the proper amount of AA (0.5, 0.1, and 0.2 g), cross-linking agent BIS (0.03 g, 3.0 wt %), and H_2O (90 mL) were added to a 250 mL round-bottom flask with a mechanical stirrer under nitrogen atmosphere. To form the emulsion, the mixture was stirred with a rotation speed of 500 rpm. After 30 min, KPS (0.05 g, 5.0 wt %) was dissolved in 10 mL H_2O and slowly added to the reaction flask. The transparent emulsion became turbid within 20 min after adding KPS. The continuous polymerization reaction was conducted for 5 h at 75 °C. After polymerization, the product was purified in a dialysis tube (molecular weight cutoff at 12 kDa; Sigma-Aldrich) with 1000 mL of deionized water for 1 week. The deionized water was exchanged at intervals of 24 h. All of the characterizations and tests, microgel dispersions with a concentration of 0.1 wt % were used.

Synthesis of Positively Charged PMETAC Brushes

Polymer brushes were prepared by versatile SI-ATRP.[24] Initiator modified Si substrates were prepared by vapor deposition of silane initiator under vacuum. METAC monomer (4 mL, 80% in water) was dissolved in 4 mL water/methanol (v:v = 2:1) mixed solvent at room temperature and degassed with N_2 for 10 min. Then, bipyridyl (80 mg) and CuBr (40 mg) were added to into the Schlenk tube and purged with N_2 flow again, the mixture was stirred under N_2 for 15 min until a homogeneous dark-brown solution formed. In the final, initiator modified substrates were put into a Schlenk tube with N_2 protection. After polymerization for 1 h, substrates were taken out and rinsed with pure water and methanol, then dried under a flow of nitrogen.

Characterization of P(NIPAm-AA) Microgels

FT-IR spectrum was obtained on a Perkin-Elmer Transform Infrared Spectrometer (PerkinElmer, Massachusetts, USA). ^1H

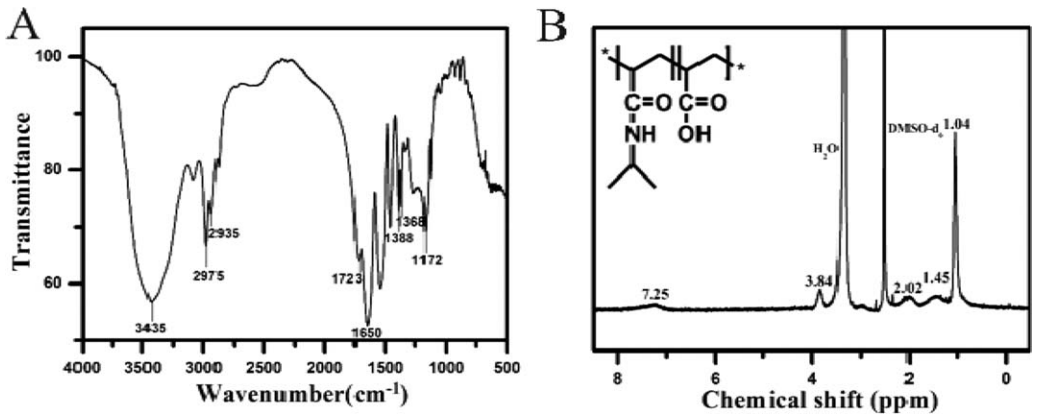

Figure 2. (A) FT-IR spectrum of P(NIPAm-AA)$_{2:1}$ microgels and (B) ^{1}H NMR spectrum of P(NIPAm-AA)$_{2:1}$ microgels.

NMR spectrum was recorded on a UNITY INOVA 400-MHz spectrometer (Varian, California, USA) using DMSO-d_6 as solvent. Transmission electron microscopy (TEM) images were obtained from a FEI Tecnai G2 TF20 transmission electron microscope with a field emission gun operating at 200 kV.

Hydrodynamic diameters (D_h) and ζ-potential of microgels were measured by dynamic light-scattering technique and Doppler laser electrophoretic system, respectively, that use a particle size analyzer (Zetasizer Nano ZS; Malvern Instruments, UK) equipped with a 632.8-nm He–Ne laser. Thickness of the polymer layer was measured using a spectroscopic ellipsometer (Gaertner model L116E) equipped with a He–Ne laser source (λ = 632.8 nm) at a fixed angle of incidence of 50°. The refractive index of the polymer film was 1.45.

The microgel particles adsorption assay was acquired by Quartz Crystal Microbalance with dissipation measurements (QCM-D) at 25 °C. Commercially available (QSX-301, QSense) gold-coated quartz chips were used. The electrode was fixed in a special apparatus, so that only one side of the electrode was in contact with the solutions. The decrease in the resonance frequency, Δf, was measured for each adsorption step. The mass of the adhering layer is calculated by using the Sauerbrey relation:

$$\Delta m = -C\frac{1}{n}\Delta f$$

Where Δf is the measured resonance frequency decrease (Hz), n is the fundamental crystal frequency (5 Hz), C is the 17.7 ng/(Hz cm^2) for a 5-MHz quartz crystal, and Δm is the mass change (ng/cm^2).

Tapping mode atom force microscope (AFM) (Agilent 5500) was employed to characterize the morphology of dried microgel particles adsorbed on the wafer. The scanning size of all images shown in work was 20 × 20 μm^2. Cantilever with a nominal resonance frequency 65 kHz (air) was operated in tapping mode. The experiment was performed by immersing brushes modified wafers into a solution of microgels for 30 min and then washed the wafers with water and dried under a flow of nitrogen.

Friction Test

The tribological properties tests were performed on a conventional pin-on-disk reciprocating tribometry (UMT-2; CETR) by recording the friction coefficient (μ) at different sliding conditions. Elastomeric poly(dimethylsiloxane) (PDMS) hemisphere with a diameter of 5 mm was employed as a pin in water. The distance of one sliding cycle was 10 mm, and the friction coefficient was determined by dividing the friction force by applied normal load through software on the PC. At least, three friction tests were repeated for each sample to get average value. The friction tests were performed by injecting 40 μL microgels solution on the interface between PDMS ball and brushes modified wafer.

RESULTS AND DISCUSSION

Microgel Synthesis and Characterization

First of all, the as-prepared P(NIPAm-AA) microgels were characterized using FT-IR and NMR. As shown in Figure 2, the chemical structure of the P(NIPAm-AA)$_{2:1}$ microgels was well-defined. Figure 2A shows the FT-IR spectrum of the microgels, where the appearance of the following signals indicates qualitatively the successful copolymerization of NIPAm and AA. The strong and wide absorption bands at 3600–3200 and 2975–2935/cm were assigned to the stretching vibration of N−H groups and C—H in methyl and methylene, respectively. The peaks at 1723 and 1650/cm were the characteristic absorption of acid carbonyl and amide carbonyl, respectively. The double peaks at 1388 and 1368/cm were attributed to the coupling vibration split absorption of the two methyl groups in —CH(CH$_3$)$_2$. The strong peak at 1172/cm was to the C—O in acid linkage. The ^{1}H NMR spectrum of the copolymer P(NIPAm-AA)$_{2:1}$ microgels shown in Figure 2B also confirms the microgel successful preparation, where all the peaks can be accurately identified. The peaks were assigned as follows: δ = 7.25 (1H, —NH—), 3.84 [1H, —CH (CH$_3$)$_2$], 2.02 (2H, —CH—C═O), 1.45 (4H, —CH$_2$—CH—), and 1.04 [6H, —CH(CH$_3$)$_2$]. In addition, the peak at 2.50 ppm was assigned to DMSO-d_6.

Subsequently, the morphology of microgels was observed via TEM. As shown in Figure 3, the as-prepared P(NIPAm-AA) microgels by surfactant-free emulsion polymerization had a spherical structure and exhibited very good polydispersity, and the mean diameter was 460 ± 20, 440 ± 30, and 410 ± 30 nm for P(NIPAm-AA)$_{2:1}$, P(NIPAm-AA)$_{5:1}$, and P(NIPAm-AA)$_{10:1}$, respectively.

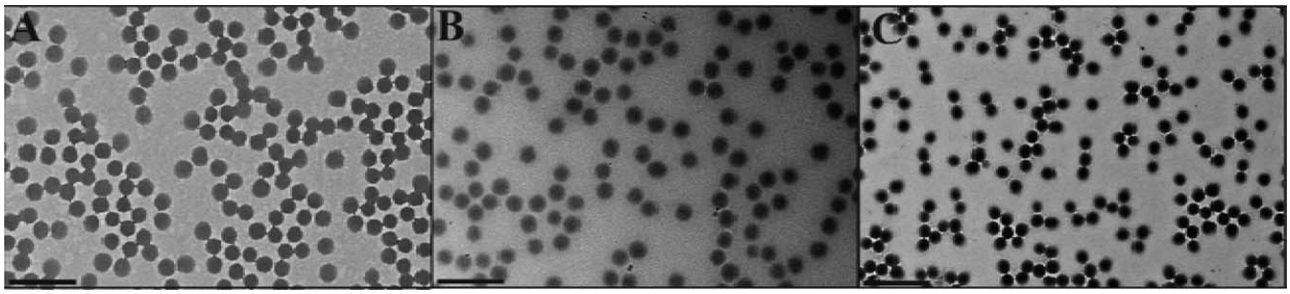

Figure 3. TEM images of (A) P(NIPAm-AA)$_{2:1}$, (B) P(NIPAm-AA)$_{5:1}$, and (C) P(NIPAm-AA)$_{10:1}$. The scale bar is 2 μm.

Table I. The D_h and ζ-potential analysis results of microgels

Microgels	NIPAm:AA (w/w)	ζ (mV)	D_h (nm) (25 °C)
P(NIPAm-AA)$_{2:1}$	2:1	−15.2 ± 0.3	1229
P(NIPAm-AA)$_{5:1}$	5:1	−12.3 ± 0.5	1075
P(NIPAm-AA)$_{10:1}$	10:1	−7.28 ± 0.3	875.7

Then, the hydrodynamic diameter (D_h) and ζ-potential of the P(NIPAm-AA) microgels in aqueous media were investigated by dynamic light scattering technique and Doppler laser electrophoretic system respectively. As shown in Table I, the ζ-potential of microgels became more negative with the increase content of AA. As was expected, the hydrodynamic diameter (D_h) of the microgels at 25 °C increased with the increasing AA content due to the increasing electrostatic repulsion between the polymer chains and the increase in the osmotic pressure.[25–27] Additionally, the hydrodynamic size and ζ-potential distribution exhibited a single peak, indicating a good dispersibility of the resultant composites in water.

The kinetics of microgels adsorption on PMETAC brushes was monitored using quartz crystal microbalance with dissipation measurement (QCM-D). Figure 4A shows the changes in the frequency of PMETAC brushes coated quartz chip during adsorption process. First, a rapid decrease in frequency was observed, which indicated that the total mass of the brush increased and plenty of microgels adsorbed on the surface of polymer brushes. Obviously, the adsorbed capacity of P(NIPAm-AA)$_{2:1}$ microgels on brushes was much higher than the other two. After rinsing with water, part of dissociative or physical absorbed microgels were washed off, while the initially adsorbed microgels through electrostatic interaction were remained on the surface. The eventual frequency decrease (Δf) indicated that microgels adsorption capacity increased as the order of P(NIPAm-AA)$_{2:1}$ > P(NIPAm-AA)$_{5:1}$ > P(NIPAm-AA)$_{10:1}$. As shown in Figure 4B, the mass of adsorption for P(NIPAm-AA)$_{2:1}$, P(NIPAm-AA)$_{5:1}$, and P(NIPAm-AA)$_{10:1}$ was 885, 637.2, and 495.6 ng/cm^2, respectively. According to the results, it can be concluded that the charge of the microgels controls the adsorption capacity of microgels and the higher charge density means stronger absorption ability.

The surface topography of polymer brushes after the adsorption of microgels was further characterized using AFM. As shown in Figure 5, plenty of microgels adsorbed on the surface of polymer brushes and the adsorption capacity increased as the order of P(NIPAm-AA)$_{2:1}$ P(NIPAm-AA)$_{5:1}$ > P(NIPAm-AA)$_{10:1}$. Moreover, the absorption density on the interface for the three kinds of microgels was 10,200, 5250, and 3500/mm^2, respectively. In other words, the surface coverage increased with the increase in surface charge density of the microgels. As can be seen in Figure 5, the lateral dimension of the dry microgels was found to be between 500 and 600 nm for the three samples. However, the corresponding 3D views showed the average height of the dry microgel particles was no more than 200 nm, indicating shrinkage mainly occurred perpendicular to the surface and not in the lateral direction, which is consistent with previous studies.[28,29]

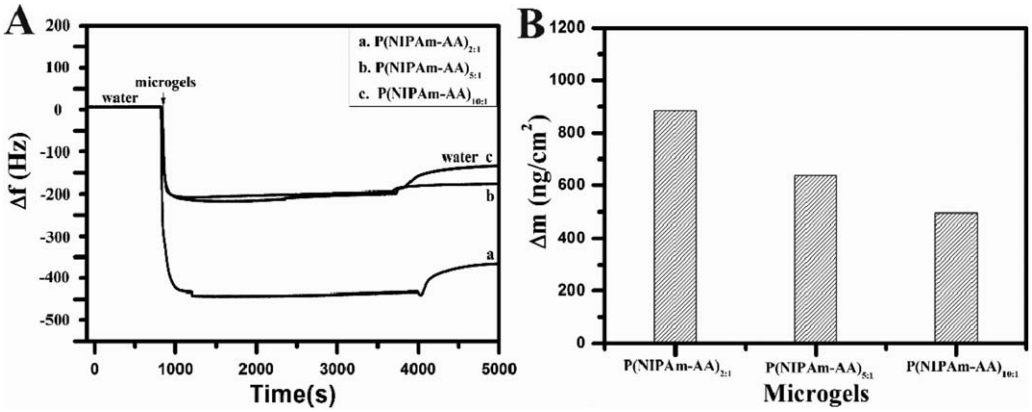

Figure 4. (A) Changes in frequency of QCM chip modified with PMETAC brushes after adsorption of microgels (0.1 wt %); (B) The adsorption masses of microgels on QCM chips modified with PMETAC brushes.

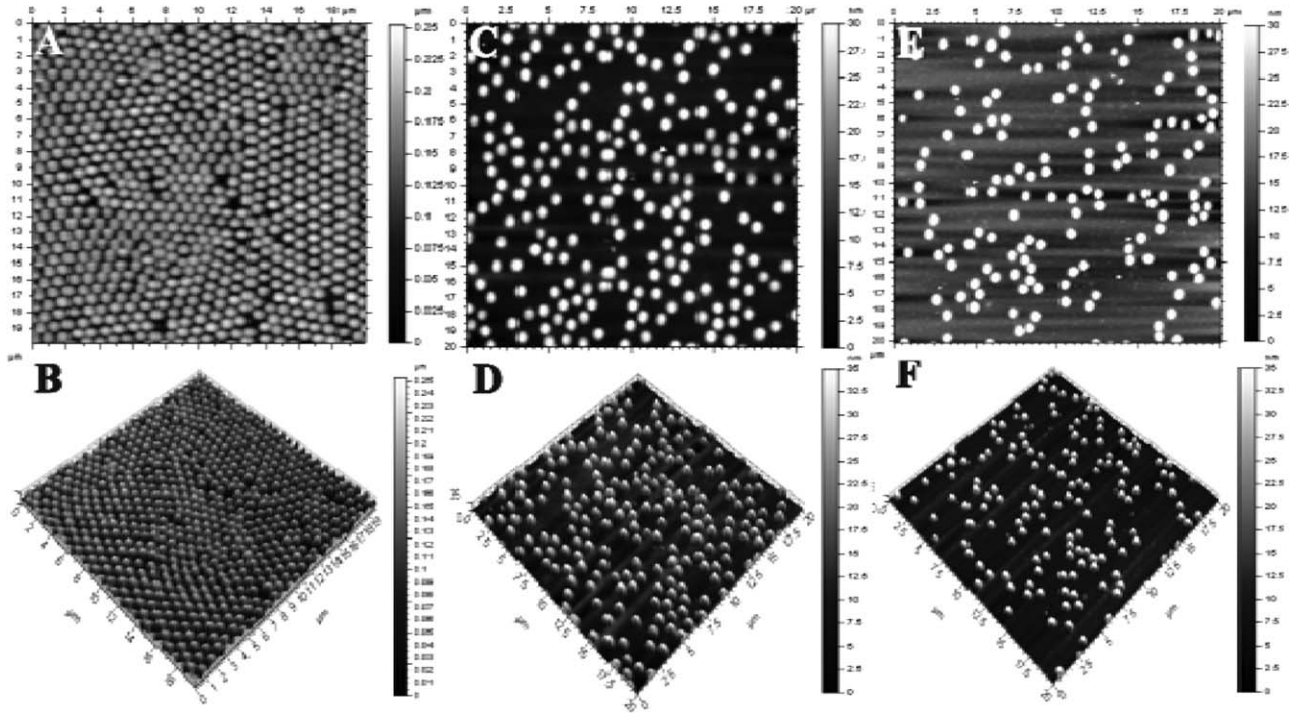

Figure 5. Morphology characterization of microgels (0.1 wt %) after adsorbed on PMETAC brushes and the corresponding 3D views. (A,B) P(NIPAm-AA)$_{2:1}$; (C,D) P(NIPAm-AA)$_{5:1}$; and (E,F) P(NIPAm-AA)$_{10:1}$. The image size is 20 μm × 20 μm.

Investigation of the Electrostatic Interaction between Polymer Brushes and Negatively Charged Microgels

Polyelectrolyte chains will present a strongly stretched conformation in pure water, due to the electrostatic repulsion between neighboring charged groups.[30] Surfaces covered with PMETAC brushes (about 20 nm in thickness) exhibited extremely low friction coefficient in water ($\mu \approx 0.01$), indicating strong swelling of these brushes in water.[31,32] Herein, a series of P(NIPAm-AA) microgels were synthesized, and the electrostatic interaction between cationic PMETAC brushes and negatively charged microgels was explored. This kind of strong electrostatic attraction made plenty of microgels adsorb on the surface of polymer brushes and microgels with different charge density may make different influence on interfacial friction.

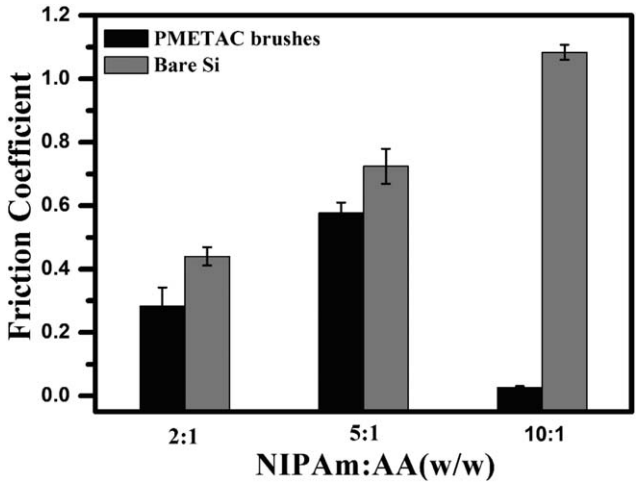

Figure 6. Friction coefficients of microgels (0.1 wt %) with various amounts of acrylic acid on PMETAC brushes and bare silicon surfaces. The friction test was carried out by sliding a silicone elastomer ball at a sliding velocity of 2 × 10^{-3} m/s under the load of 0.5 *N*.

As shown in Figure 6, the friction coefficients of interface after adsorption were 0.28, 0.58, and 0.027 for P(NIPAm-AA)$_{2:1}$, P(NIPAm-AA)$_{5:1}$, and P(NIPAm-AA)$_{10:1}$, respectively. On the basis of the hydration mechanism illustrated in Figure 1, water molecules could form hydrated layer surrounding the charges, which can support high pressures.[33,34] For P(NIPAm-AA)$_{2:1}$ and P(NIPAm-AA)$_{5:1}$ microgels, the weaker hydration capability compared to that of polymer brushes led to a concomitant increase in friction of interface, while P(NIPAm-AA)$_{2:1}$ microgels with more AA presented a lower friction attributed to the stronger hydration capability. In terms of P(NIPAm-AA)$_{10:1}$ microgels, due to the lower charge density induced weaker adsorptive strength with PMETAC brushes, they could be sheared off easily under the load of 0.5 *N* and swelled again to present a lower friction of interface. Then we studied the friction coefficients of bare silicon surfaces after in situ injection of microgels. The friction coefficients of interface were 0.44, 0.72, and 1.08 for P(NIPAm-AA)$_{2:1}$, P(NIPAm-AA)$_{5:1}$, and P(NIPAm-AA)$_{10:1}$, respectively. Such a high friction coefficient was the result of hydrophobic silicon that made it difficult for microgels to form stable hydration layers.[35]

Figure 7A shows friction coefficients of P(NIPAm-AA)$_{2:1}$ microgels on PMETAC brushes under different frequencies. As the frequency increased from 0.2 to 5 Hz, the friction coefficient decreased gradually from 0.28 to 0.03. The lower friction at high frequency indicated that microgels have been sheared off

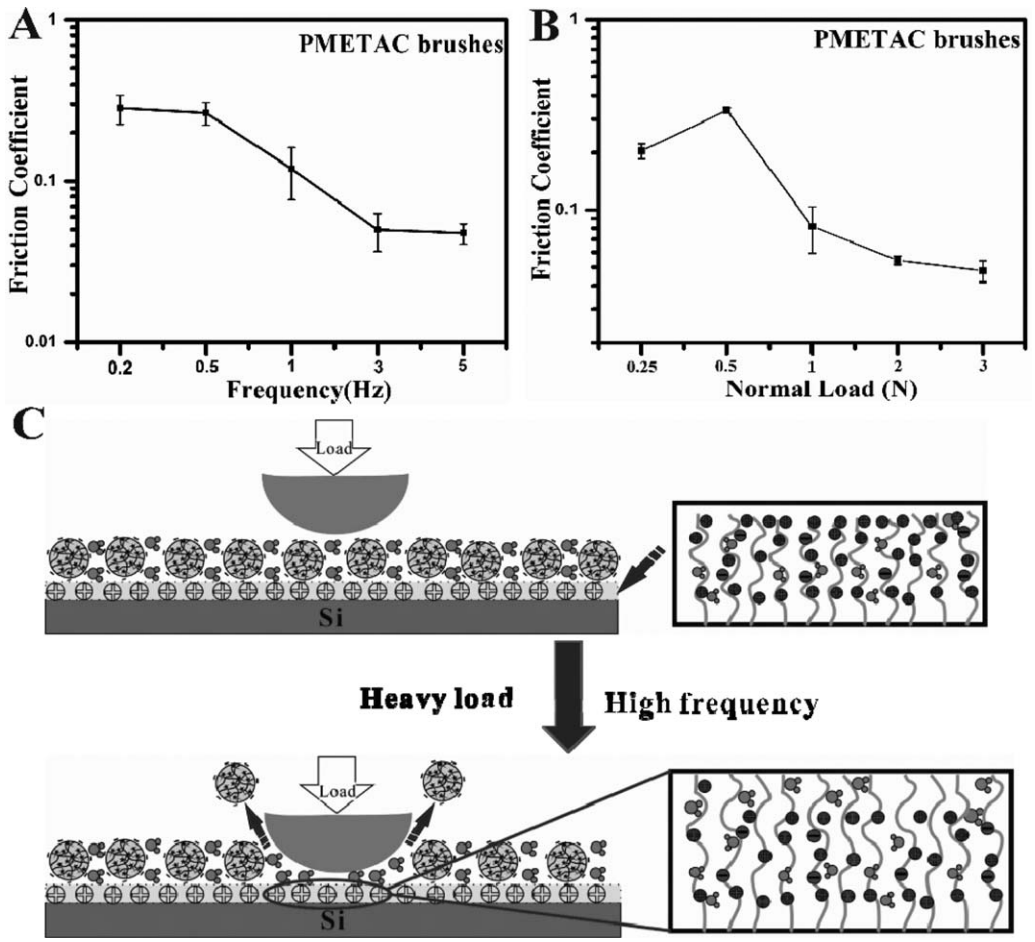

Figure 7. (A) Friction coefficients of P(NIPAm-AA)$_{2:1}$ microgels (0.1 wt %) on PMETAC brushes with different frequencies under the normal load of 0.5 *N*. (B) Friction coefficients of P(NIPAm-AA)$_{2:1}$ microgels (0.1 wt %) on PMETAC brushes with different normal load under the frequency of 0.2 Hz. (C) Schematic diagram illustrating the friction process for heavier load or higher frequency.

and the rate of adsorption was lower than the shear velocity. Later, we studied the friction coefficients of P(NIPAm-AA)$_{2:1}$ microgels on PMETAC brushes under different normal load (Figure 7B). As the normal load increased from 0.25 to 3 *N*, the friction coefficient first increased and then decreased. The increase of friction was due to the heavier load that made the deformation of microgels more serious and decreased the lubricating effect. However, when the normal load increased to 2 *N*, the friction coefficient decreased to 0.04, indicating that microgels have been sheared off by the higher shear force. Thus, it can be concluded that P(NIPAm-AA)$_{2:1}$ microgels could be sheared off by heavier load or higher frequency and made PMETAC brushes swell again and thus presented a lower friction of interface. Relative schematic diagram is shown in Figure 7C.

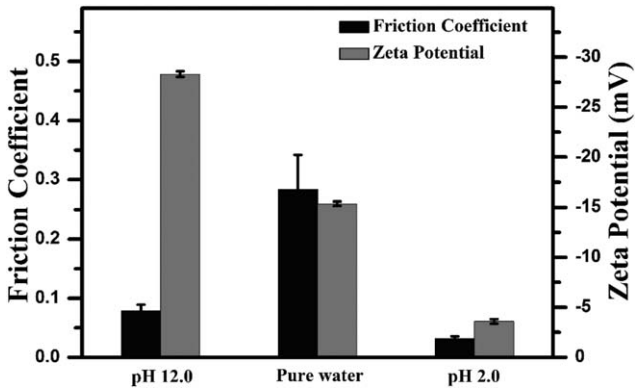

Figure 8. Friction coefficients of P(NIPAm-AA)$_{2:1}$ microgels (0.1 wt %) on PMETAC brushes under different pH.

Furthermore, we investigated the effect of P(NIPAm-AA)$_{2:1}$ microgels with different pH on the friction of interface. The microgel suspensions were vigorously shaken for 24 h to redisperse the freeze-dried microgel powder in solution. The pH adjustment of the particle suspensions was accomplished by using two different buffer solutions: (1) pH = 2.0, (2) pH = 12.0 and the ζ-potential of this two kind microgels were −3.76 ± 0.3 and −28.5 ± 0.2 mV, respectively. Clearly, partially protonation of carboxylic acid groups at low pH led to lower charge density and higher ζ-potential, conversely, the high pH accelerated the dissociation of AA that led to higher charge density. Figure 8 shows changes in the friction coefficient of P(NIPAm-AA)$_{2:1}$ microgels on PMETAC brushes under different pH. Comparing to that in pure water, the lower friction (≈0.078) at pH 12.0 indicated that

the higher charge density led to a stronger hydration capability of microgels. While the lower friction (≈0.032) at pH 2.0 was due to the weaker adsorption that made microgels be sheared off, so that PMETAC brushes stretched again and presented better lubricating effect.

CONCLUSIONS

Monodisperse microgel particles have been prepared by copolymerization of NIPAm and AA via surfactant-free emulsion polymerization, and the tribological behavior and electrostatic self-assemble of the as-prepared microgels on polymer brushes were investigated in detailed. For cationic PMETAC brushes, negative charged P(NIPAm-AA) microgels adsorbed on the surfaces of brushes due to the electrostatic interaction, and more AA content means higher charge density and stronger absorption ability. In regard to P(NIPAm-AA)$_{2:1}$ and P(NIPAm-AA)$_{5:1}$ microgels, since microgels own weaker hydration capability than the polymer brushes, the friction of interface increased and the microgels could be sheared off under the load of 1 *N*. Due to the weak adsorption to substrate, P(NIPAm-AA)$_{10:1}$ microgels could be sheared off easily under the load of 0.5 *N* and made PMETAC brushes stretch again, thus a lower friction of interface was obtained. Furthermore, the P(NIPAm-AA)$_{2:1}$ microgels exhibited good lubrication effect in high pH solution owing to the high hydration of deprotonated carboxylic acid groups.

Herein, the microgels were electrostatically assembled into densely packed monolayer on silicon wafers using polyelectrolyte brushes as an anchor group. This kind of attachment provides guidance for using these linking groups on all kinds of substrates, such as most metal, glass and many organic surfaces. Moreover, the highly stable microgels monolayers on charged surfaces derived from electrostatic adsorption further increase their versatility. We believe that thermoresponsive PNIPAm microgel films will have a range of important applications in cell culture and medical devices.

ACKNOWLEDGMENTS

This study was financially supported by NSFC (21434009, 21204095, and 51573199) and Youth Innovation Promotion Association CAS.

REFERENCES

1. Horigome, K.; Suzuki, D. *Langmuir* **2012**, *28*, 12962.
2. Heyes, D. M.; Brańka, A. C. *Soft Matter* **2009**, *5*, 2681.
3. Wiedemair, J.; Serpe, M. J.; Kim, J.; Masson, J. F.; Lyon, L. A.; Mizaikoff, B.; Kranz, C. *Langmuir* **2007**, *23*, 130.
4. Seiffert, S. *Angew Chem. Inter. Ed.* **2013**, *52*, 11462.
5. Chen, M.; Zhou, L.; Guan, Y.; Zhang, Y. *Angew. Chem. Int. Ed.* **2013**, *52*, 9961.
6. Schmidt, S.; Hellweg, T.; Klitzing, R. V. *Langmuir* **2008**, *24*, 12595.
7. Hirokawa, Y.; Tanaka, T. *J. Chem. Phys.* **1984**, *81*, 6379.
8. Wong, J. E.; Diez-Pascual, A. M.; Richtering, W. *Macromolecules* **2009**, *42*, 1229.
9. Kleinen, J.; Klee, A.; Richtering, W. *Langmuir* **2010**, *26*, 11258.
10. Kwon, I. C.; Bae, Y. H.; Kim, S. W. *Nature* **1991**, *354*, 291.
11. Sierra, M. B.; Maldonado, V. A.; Las Nieves, F. J.; Fernandez-Barbero, A. *J. Nanosci. Nanotechnol.* **2015**, *15*, 3584.
12. Liu, F.; Urban, M. W. *Prog. Polym. Sci.* **2010**, *35*, 3.
13. Tsai, H. Y.; Vats, K.; Yates, M. Z.; Benoit, D. S. *Langmuir* **2013**, *29*, 12183.
14. Wu, Y.; Cai, M.; Pei, X.; Liang, Y.; Zhou, F. *Macromol. Rapid Commun.* **2013**, *34*, 1785.
15. Wu, Y.; Pei, X. W.; Wang, X. L.; Liang, Y. M.; Liu, W. M.; Zhou, F. *NPG Asia Mater.* **2014**, *6*, 136.
16. Sun, T.; Wang, G.; Feng, L.; Liu, B.; Ma, Y.; Jiang, L.; Zhu, D. *Angew. Chem. Int. Ed.* **2004**, *43*, 357.
17. Chang, D. P.; Dolbow, J. E.; Zauscher, S. *Langmuir* **2007**, *23*, 250.
18. Serpe, M. J.; Jones, C. D.; Lyon, L. A. *Langmuir* **2003**, *19*, 8759.
19. Schmidt, S.; Motschmann, H.; Hellweg, T.; Klitzing, V. R. *Polymer* **2008**, *49*, 749.
20. Guan, Y.; Zhang, Y. *Soft Matter* **2011**, *7*, 6375.
21. Schmidt, S.; Zeiser, M.; Hellweg, T.; Duschl, C.; Fery, A.; Möhwald, H. *Adv. Funct. Mater.* **2010**, *20*, 3235.
22. Jones, D. M.; Brown, A. A.; Huck, W. T. S. *Langmuir* **2002**, *18*, 1265.
23. Husseman, M.; Malmström, E. E.; McNamara, M.; Mate, M.; Mecerreyes, D.; Benoit, D. G.; Hedrick, J. L.; Mansky, P.; Huang, E.; Russell, T. P. *Macromolecules* **1999**, *32*, 1424.
24. Li, B.; Yu, B.; Ye, Q.; Zhou, F. *Acc. Chem. Res* **2014**, *48*, 229.
25. Kratz, K.; Hellweg, T.; Eimer, W. *Colloids Surf. A* **2000**, *170*, 137.
26. Burmistrova, A.; Richter, M.; Eisele, M.; Uzum, C.; Klitzing, V. R. *Polymer* **2011**, *3*, 1575.
27. Hu, L.; Chen, M.; Fang, X.; Wu, L. *Chem. Soc. Rev.* **2012**, *41*, 1350.
28. Nerapusri, V.; Keddie, J. L.; Vincent, B.; Bushnak, I. A. *Langmuir* **2006**, *22*, 5036.
29. Sorrell, C. D.; Lyon, L. A. *J. Phys. Chem. B* **2007**, *111*, 4060.
30. Farhan, T.; Azzaroni, O.; Huck, W. T. S. *Soft Matter* **2005**, *1*, 66.
31. Kobayashi, M.; Terada, M.; Takahara, A. *Faraday Discuss.* **2012**, *156*, 403.
32. Kobayashi, M.; Takahara, A. *Chem. Record.* **2010**, *10*, 208.
33. Klein, J. *Friction* **2013**, *1*, 1.
34. Liu, G.; Wang, X.; Zhou, F.; Liu, W. *ACS Appl. Mater. Interfaces* **2013**, *5*, 10842.
35. Lee, S.; Spencer, N. D. *Tribol. Int.* **2005**, *38*, 922.